Developmental Biology 334 (2009) 84–96

Contents lists available at ScienceDirect

Developmental Biology

journal homepage: www.elsevier.com/developmentalbiology

Origin of the prechordal plate and patterning of the anteroposterior regional specificity of the involuting and extending archenteron roof of a urodele, *Cynops pyrrhogaster*

Teruo Kaneda *, Yujiro Iwamoto, Jun-ya Doi Motoki

Department of Bioengineering and Advanced Course for Bioengineering, Yatsushiro National College of Technology, 2627, Hirayama Shin-Machi, Yatsushiro 866-8501, Japan

ARTICLE INFO

Article history:
Received for publication 16 January 2009
Revised 12 June 2009
Accepted 9 July 2009
Available online 28 July 2009

Keywords:
Gastrulation movement
Notochord induction
Anteroposterior regional specification
Archenteron roof
Cynops pyrrhogaster
Urodele

ABSTRACT

We analyzed the notochord formation, formation of the prechordal plate, and patterning of anteroposterior regional specificity of the involuting and extending archenteron roof of a urodele, *Cynops pyrrhogaster*. The lower (LDMZ) and upper (UDMZ) domains of the dorsal marginal zone (DMZ) of the early gastrula involuted and formed two distinct domains: the anterior fore-notochordal endodermal roof and the posterior domain containing the prospective notochord. *Cygsc* is expressed in the LDMZ from the onset of gastrulation, and the *Cygsc*-expressing LDMZ planarly induces the notochord in the UDMZ at the early to mid gastrula stages. At the mid to late gastrula stages, part of the *Cygsc*-expressing LDMZ is confined to the prechordal plate. On the other hand, *Cybra* expression only begins at mid gastrula stage, coincident with notochord induction at this stage. Anteroposterior regional specificity of the neural plate was patterned by the posterior domain of the involuting archenteron roof containing the prospective notochord at the mid to late gastrula stages. *Cynops* gastrulation thus differs significantly from *Xenopus* gastrulation in that the regions of the DMZ are specified from the onset of gastrulation, while the equivalent state of specification does not occur in *Cynops* until the middle of gastrulation. Thus we propose that *Cynops* gastrulation is divided into two phases: a notochord induction phase in the early to mid gastrula, and a neural induction phase in the mid to late gastrula.

Introduction

Gastrulation is a set of evolutionarily conserved morphogenetic movements in the early development of a wide variety of vertebrates. In amphibians, the cells of the dorsal marginal zone (DMZ) involute through the blastopore by convergent-extension and involution movements to form the archenteron roof (ARF). By this process, progeny cells of the lower (future anterior) and upper (future posterior) DMZ spatially and temporally interact with each other and with the overlying presumptive ectoderm to form the central nervous system (CNS). Two major inductive interactions are required in this process. One is mesoderm induction in the DMZ and establishment of the anteroposterior and dorsoventral regional specificity of the induced mesoderm. The other is neural induction, in which induced and regionally specified mesoderm interacts with the presumptive ectoderm during gastrulation. Thus, the early patterning of the CNS involves a complex set of spatial and temporal inductions, morphogenetic movements and regional interactions.

Using urodelean embryos, Mangold (1933) proposed separate set of organizers that induce the head and the trunk–tail neural structures. On the other hand, in an activation and transformation model, Nieuwkoop et al. (1952) proposed that anteroposterior CNS patterning requires spatial and temporal combination of the two signals emanated from involuting ARF: an activation signal and a transformation signal. However, it remains to be resolved when and how these regional specificities of the ARF are established, when is neural induction initiated, and what are the cellular sources of the neural inducing signals (Wilson and Edlund, 2001). To explain the origin of the regional specification of the ARF, Vodicka and Gerhart (1995) and Zoltewicz and Gerhart (1997) analyzed regional gene expression pattern of the *Xenopus* early gastrula DMZ. They demonstrated that the DMZ of the *Xenopus* early gastrula was divided into a *gsc*-expressing domain in the lower half, *Xnot* in the upper half, and *Xbra* in the middle, partially overlapping both *gsc* and *Xnot*. Winklbauer and Schürfeld (1999) further demonstrated that in *Xenopus* stage 10- the DMZ was composed of a lower *gsc*-expressing domain, an upper *Xbra*-expressing domain, and the internal *cerberus*-expressing domain, and these domains involuted and extended while retaining their spatial integrity. Thus it has been proposed that in *Xenopus* the anteroposterior regional characteristics of the ARF are patterned in the early gastrula DMZ prior to the onset of gastrulation (see reviews, Harland and Gerhart, 1997; Gerhart, 2001). These earlier

* Corresponding author. Department of Bioengineering, Yatsushiro National College of Technology, 2627, Hirayama Shin-Machi, Yatsushiro 866-8501, Japan. Fax: +81 965 53 1389.
E-mail address: kaneda@as.yatsushiro-nct.ac.jp (T. Kaneda).

0012-1606/$ – see front matter © 2009 Elsevier Inc. All rights reserved.
doi:10.1016/j.ydbio.2009.07.032

reports indicate that interactions between and within these domains are crucial for the regional specificity of the DMZ in *Xenopus*, although the location of these domains, and their spatial and temporal functions in anteroposterior neural patterning, during gastrulation have not been fully elucidated. On the other hand, it has been reported that specification of the early gastrula DMZ is not yet established and the early gastrula DMZ is quite labile (Kaneda and Suzuki, 1983; Saha and Grainger, 1992; Grunz, 1993; Sakaguchi et al., 2002). Furthermore, the presence of notochord inducing signals within the DMZ or suprablastoporal endodermal epithelium has been demonstrated in *Xenopus* and *Bufo* gastrula, even up to the late gastrula stage (Stewart and Gerhart, 1991; Shin and Keller, 1992; Domingo and Keller, 1995; Lane and Keller, 1997; Manes and Casal, 1997).

In comparison with urodelean embryos, *Xenopus* has unique features of its germ layer structure and mode of gastrulation. The *Xenopus* DMZ is a multilayered structure that undergoes an internal gastrulation prior to the onset of gastrulation, in which mesoderm involution takes place independently of archenteron involution (Nieuwkoop and Florschütz, 1950; Keller, 1976). In contrast, the early gastrula DMZ of urodeles has a monolayered structure, and all the constituents of the future ARF are located on the egg surface (Vogt, 1929; Hama, 1978; Delarue et al., 1992; Nieuwkoop, 1996; Imoh et al., 1998; Johnson et al., 2003). During gastrulation, they synchronously initiate the internal and external morphogenetic steps. These differences in germ layer structure and the mode of gastrulation will made it difficult to compare similarities and differences in basic morphogenetic events, such as the mesoderm and neural induction processes, between anurans and urodeles (Eagleson, 1996; Nieuwkoop, 1996).

We previously demonstrated that the early gastrula DMZ of *Cynops pyrrhogaster* is spatially bisected into a lower and upper DMZ (LDMZ and UDMZ) in its fate, autonomy for cell differentiation, gene expression and organizing activities (Kaneda et al., 2002). Because the LDMZ, which is the suprablastoporal endoderm region that is fated mainly to become pharyngeal endoderm, is known to induce a complete secondary axis (Yamamoto and Suzuki, 1994; Imoh et al., 1998), and this activity is based on its potent notochord inducing activity, we have proposed that the LDMZ is essential for initiating the sequence of events that leads to the formation of the anteroposterior body pattern (Kaneda et al., 2002; Sakaguchi et al., 2002). However, the interactions between the LDMZ and UDMZ during gastrulation, when the anteroposterior regional specification of the ARF is established, and when and where neural induction is initiated, have yet to be elucidated. In this study, we found that the *Cynops* gastrula ARF comprises two spatially distinct domains in its gene expression, organizing activities and self-differentiation. The regional natures of the ARF are characterized by planar interaction between LDMZ and UDMZ. In conclusion, we propose that *Cynops* gastrulation is divided into two phases, a notochord induction phase at early to mid gastrula, and a neural induction phase at mid to late gastrula.

Materials and methods

Embryos

Embryos of the Japanese newt, *C. pyrrhogaster* (diameter: 2.1–2.3 mm) were developed at 20 °C. Very early gastrulae, characterized by a pigment line formed by the accumulation of bottle cells, were selected and designated as stage 11 (normal table of *C. pyrrhogaster* according to Okada and Ichikawa, 1947). The DMZ was defined as the area between the pigment line and the limit of involution along the dorsal midline, as described previously (Kaneda and Hama, 1979; Kaneda et al., 2002). Staging of the early to late gastrulae was performed according to the hours of development from stage 11 and the length of the ARF (Kaneda and Hama, 1979). Involution of the ARF was almost completed in the late gastrula (stage 13c, about 24 h from stage 11, length of ARF approximately 3.0 mm). Early neurulae (stages 15–16), neural-plate stage neurulae (stage 18) and early tailbud (stages 22–23) embryos were also used.

Microsurgery and cell culture

Microsurgery and cell culture were performed in Holtfreter's solution (HFS, adjusted to pH 7.4 with sodium bicarbonate) containing 30 mg/L gentamicin. The egg capsule was removed by incubating the embryos in 1% thioglycol (pH 9.5 with NaOH) for 50–80 s, then washing them several times with HFS. Stage 13c late gastrulae were dissected and the ARF was peeled away from the overlying prospective neuroectoderm, then anteroposteriorly divided into six parts of the same size (0.5×0.5 mm). The organizing activity of each part of the ARF was analyzed by a sandwich assay method in which the part of the ARF was sandwiched with two sheets of animal cap presumptive ectoderm from stage 11 early gastrula. To achieve immediate adhesion between the ARF and the presumptive ectoderm, the explants were weighted with another embryos. After healing, the explants were cultured at 20 °C for 4 days for RNA isolation, or for 2 weeks for histological observations.

Keller sandwiches of early gastrula DMZ were also produced. The DMZ was dissected (1.0 mm width, 1.5 mm height), stripped into two and the inner surfaces fused together and weighted as described above to facilitate adhesion. To eliminate contamination of the bottle cells, the vegetal margin was in the middle portion of the LDMZ, and the animal margin was in the presumptive posterior neural plate. Each Keller sandwich was cultured for 1 or 24 h (at 24 h, the sibling embryo had reached the stage 13c late gastrula), and then fixed with MEMFA for *in situ* hybridization.

Vital dye mapping

Vital staining was performed to accurately define the position of the progeny cells of the LDMZ and UDMZ on the involuting and extending ARF. Melted 1% agar gel in distilled water was spread onto a microscope glass slide and hardened (3–4 mm in thickness). Next, the gel was soaked in 1% Nile-blue sulfate (Chroma) solution to saturate it with dye, then soaked in distilled water to remove excess dye, and air-dried. The dried Nile-blue-stained agar film was peeled off from the glass slide and cut into small pieces (0.5×0.5 mm) under a stereomicroscope.

The egg capsule was removed and embryos with an intact vitelline membrane were transferred to 10% HFS, then to a hole in a paraffin-wax filled dish where they were oriented by hair loops so that the pigment line faced uppermost. A piece of Nile-blue-stained agar film was placed in the desired position on each embryo and excess HFS was removed as soon as possible to facilitate close contact between the embryo and agar film via the vitelline membrane. The embryos were stained at room temperature for 10–20 min in a moist chamber, after which 10% HFS was carefully pipetted onto the agar film to remove it. The distance from the vegetal (future anterior) and animal (future posterior) margins of the dye mark on the embryo surface to the pigment line was measured, and individual stained embryos were developed in 10% HFS at 20 °C. The positions of the posterior and anterior margins of the dye mark were tracked during gastrulation.

Involution of the ARF becomes evident after 3 h from stage 11, so we dissected early stage 12a (6 h from stage 11), stage 12a (linear blastopore stage, 9 h from stage 11), stage 12b mid gastrula with semicircular blastopore (12 h from stage 11), stage 12c late gastrula (horseshoe-shaped blastopore, 18 h from stage 11), and stage 13c small yolk plug stage (24 h from stage 11) embryos to observe the position of the dye mark on the involuting ARF. In each series, at least 10 normally developed embryos were analyzed, and the average positions of the anterior and posterior margin of the dye at each stage were determined.

RNA isolation and reverse-transcriptase PCR (RT-PCR)

Total RNA was isolated from individual sandwich explants and whole embryos, and purified. The primers and polymerase chain reaction (PCR) conditions used for *EF1*-α were as previously described (Kaneda et al., 2002). For the region-specific neural markers, we used the *Cynops* homolog of *Otx2* (5′-AACTGCAGGAAGCAACCACCTTA-CACCGTGAA and 5′-GGAATTCTGTGCTAGGTGGTGGTGTGAACTG, Sakami et al., 2005), *engrailed* (*en-2*; 5′-ACGCGATACTCGGACAGGCC and 5′-GCTCGCTTGTTCTGGAACCA, Takabatake et al., 1996), *Pax6* (5′-TGGGCAACACCTGCCTAT and 5′-CTTTTTGCCAGCCGTGTCCC, Mizuno et al., 1997) and neural-specific *NCAM* (5′-CATTGCAGTGAATCTGTGTG and 5′-CGGGATCGTCTTGACTTCTG, Takabatake et al., 1996). We also used muscle-specific α-*actin* (5′-CTGGCACCCAGCACCATGAA and 5′-TAGGGGAGCTTTCAGGATGT, Takabatake et al., 1996). Each amplified fragment was subcloned into a pGEM-T Easy vector (Promega Co.) and sequenced to confirm the DNA sequence.

Whole-mount in situ hybridization

Embryos were fixed with MEMFA containing 3% percoll (Sigma) at 4 °C overnight, and then transferred to methanol and stored at −20 °C until use. Hybridization was carried out using the *Cynops* homologs of the *brachyury* (*Cybra*) and *goosecoid* (*Cygsc*) probes (Mizuno et al., 1997; Sone et al., 1997; Doi et al., 2000). After hybridization, embryos were post-fixed with MEMFA and then bleached in 2% H_2O_2–10% formamide under light. To observe the internal hybridization pattern, hybridized embryos were equilibrated with 1% phenol containing 20% gelatin at 37 °C (Fujisaki et al., 2000) and then sectioned at 100 μm using a vibratome.

Immunohistochemistry

The mouse monoclonal antibody, cyNot-2, which recognizes the protein antigen of *Cynops* embryonic notochord (Suzuki et al., 2002), was used to identify the developing notochord. Unlike Tor70, cyNot-2 does not react with epidermal ectoderm cells until the tailbud stage (Suzuki et al., 2002), so it is possible to specifically detect prospective notochord in late gastrula to tailbud embryos. Decapsulated embryos at the desired stage were fixed with absolute methanol at 4 °C and stored at −20 °C. They were then embedded in polyester wax (BDH Lab. Inc.) and sectioned at 15 μm. Serial sections were treated with absolute ethanol, rehydrated and immersed in the blocking solution (1% bovine serum albumin, 2% skimmed milk in phosphate-buffered saline) for 30 min, and then reacted with cyNot-2 antiserum (diluted 1:10 with blocking solution) at 4 °C overnight. After washing with the blocking solution, specimens were reacted with FITC-conjugated anti-mouse IgM (μ-chain) goat antibody (Vector Lab. Inc., diluted to 1:200 with blocking solution) for 1 h at room temperature and observed after they were washed again with blocking solution.

Cell lineage analysis and microscopy

For routine microscopy, specimens were fixed with 2% glutaraldehyde at 4 °C overnight, dehydrated through an ethanol series, and embedded in paraffin via xylene. Serial sections (8 μm) were stained with hematoxylin. For cell lineage analysis, fluorescein-dextran-

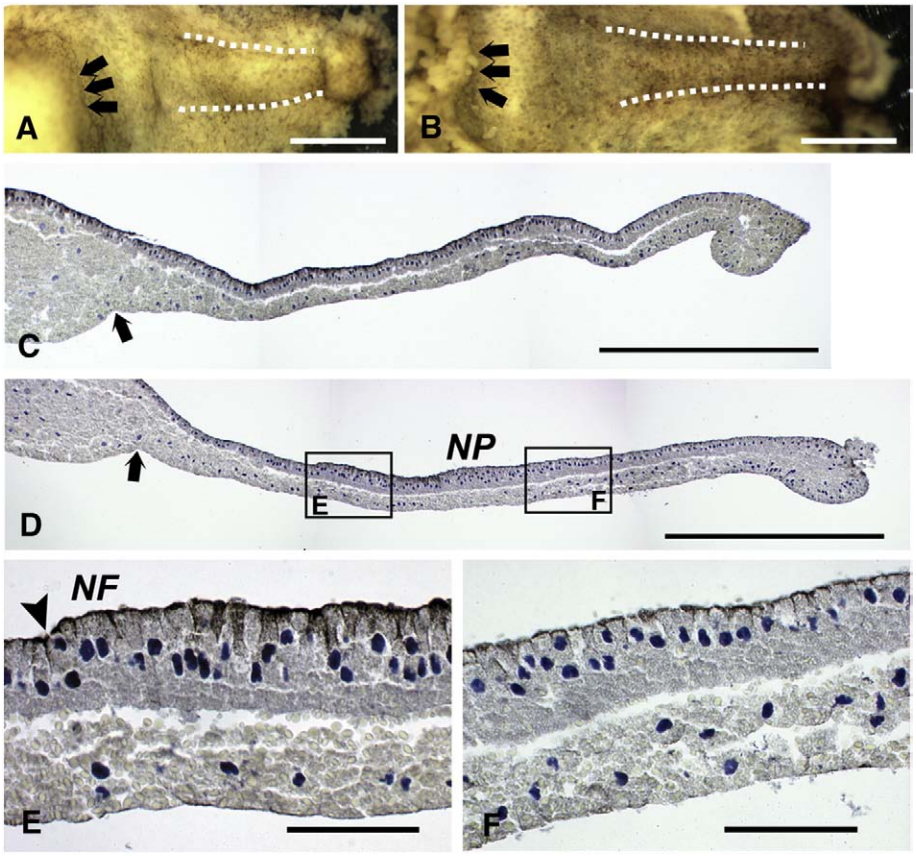

Fig. 1. Histological observation of the involuting and extending archenteron roof. Late gastrulae (stage 13c, A, C) and early neurulae (stage 15, B, D–F) were dissected to observe regional differences of the archenteron roof (ARF). Sections at the dorsal midline show that the involuting and extending ARF is a single-cell sheet, except in the most anterior pharyngeal endoderm region (C, D). The ARF loosely contacts the overlying prospective neuroectoderm. In the early neurulae, thickening of the prospective neural plate becomes evident (E, F). Bars indicate 1 mm (A–D) or 100 μm (E, F). Arrows indicate the anterior tip of the ARF. The arrowhead in panel E indicates the anterior margin of the neural fold. In all figures, left and right represent the anterior and posterior directions, respectively. NP, neural plate; NF, neural fold.

amine (FDA, Molecular Probes Inc., 20 mg/mL in 10% HFS) was injected at the 2-cell stage (10 nL/blastomere) and the labeled embryos were developed in 10% HFS until they reached stage 13c. The ARF was isolated, divided into six parts and sandwiched as described above. After cultivation for 2 weeks, the FDA-labeled specimens were fixed with Bouin's fixative, dehydrated through an ethanol series and embedded in paraffin wax. Serial sections (10 μm) were alternately mounted on separate slides. One slide was stained with hematoxylin–eosin and the other slide was examined using an epifluorescent microscope after removal of the paraffin with xylene.

Results

Histological and immunohistochemical observations of the involuting and extending ARF

During gastrulation, the cells of the DMZ involuted through the blastopore as a monolayer. Histological examination showed that the ARF was in loose contact with the overlying prospective neuroectoderm in the mid to late gastrula stages. There were no obvious regional differences at the histological level (Figs. 1A, C). Thickening of the neuroectoderm became evident from anterior to posterior, and the anterior neural fold formed at the late gastrula to early neurula stage. However, regional differences of the ARF were not clear, even at the early neurula stage (Figs. 1B, D–F).

As shown in Figs. 2A and B, cyNot-2 did not recognize the antigen at the mid to late gastrula stages. At the end of gastrulation, however, signals were observed in the middle to posterior half of the ARF, and became clearer in the early neurula stage (Figs. 2C, D). Although histological differences were not discernible (Fig. 1), immunohistochemistry showed that the late gastrula ARF is divided into two distinct domains: a middle to posterior prospective notochord half and a non-notochordal anterior half. It should be emphasized that the anterior border of the notochord was located at the center of the anterior neural plate, the cranial end of the neural groove (Figs. 2C–F). As shown later, the non-notochordal anterior half of the ARF self-

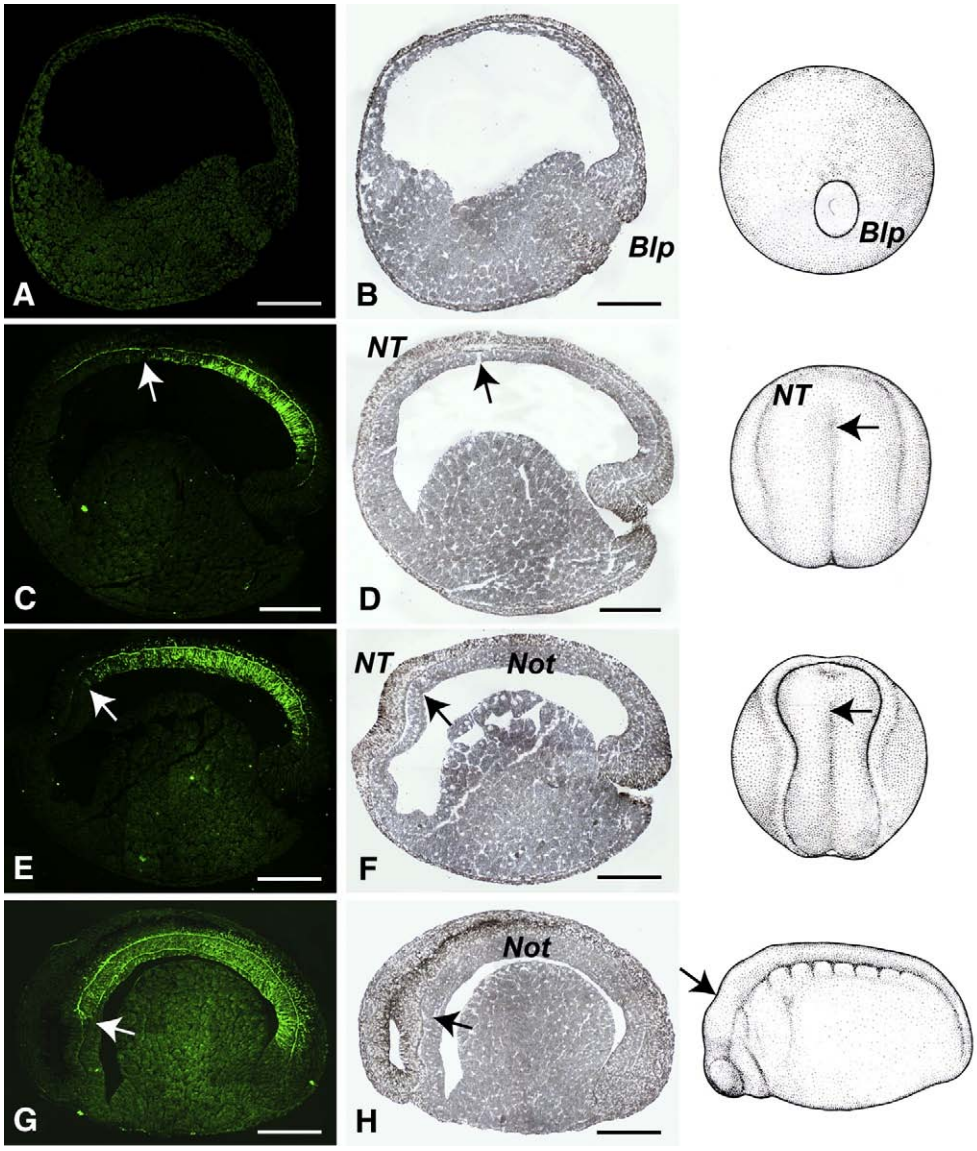

Fig. 2. Immunohistochemical identification of the development of the notochord. Notochord differentiation of the late gastrula (stage 13c, A, B), early neurula (stages 15–16, C, D), neurula (stage 18, E, F) and tailbud embryo (stages 22–23, G, H) was analyzed by cyNot-2 monoclonal antibody. CyNot-2 does not recognize the antigen in late gastrulae (A, B). At the early neurula stage (C, D), the signal can be seen in the middle to posterior portion of the ARF. The anterior end of the signal is at the center of the ARF. The signal becomes prominent from the neurula stage onward (E, F). In the neurulae, the columnar shape of the notochord becomes evident (Not). No signal was detected in the ARF located beneath the anterior forebrain part of the neural plate. At the tailbud stage (G, H), the neural plate has closed to form the brain and neural tube, and the notochordal sheath is evident. In all figures, arrows indicate the anterior tip of the notochord. Blp: blastopore; NT: thickening of the neuroectoderm; Not: notochord. Bars indicate 0.5 mm.

differentiated only into endodermal tissues, such as pharyngeal endoderm (Fig. 4). The anterior half domain of the ARF was therefore designated as the fore-notochordal endodermal roof (FNE). Signals became clearer with advancing stages, and at the neurula stage (Figs. 2E, F) the boundary between the notochord and FNE became more evident. At this stage, thickening of the anterior neural plate and neural fold became clear.

Youn et al. (1980) reported that notochord differentiation in *Xenopus* and *Ambystoma* proceeds from the posterior to the anterior ARF, whereas Suzuki et al. (2002) demonstrated that in *Cynops* notochord differentiation proceeded from the middle to the posterior. As shown in Figs. 2C and D, our results show that the cyNot-2 antigen gradually decreased from the middle junctional region between FNE and prospective notochord to the posterior end of the ARF, indicating that notochord differentiation is initiated at the junction between the FNE and prospective notochord.

Histologically, the prechordal plate was first identified as a thin, triangular region of neurula ARF, just anterior to the notochord that was underlying the forebrain part of the neural plate (Adelmann, 1932). At the neurula stage, the anterior tip of the notochord was located at the center of the anterior neural plate, but there was neuroepithelial thickening of the anterior neural plate and the neural fold lying over part of the FNE just anterior to the notochord (Figs. 2E, F). At the tailbud stage, this region was completely segregated from the notochord and lay under the floor of the forebrain (Figs. 2G, H). As shown in Fig. 5, expression of the prechordal plate marker gene (*Cygsc*) was restricted to this region, so the part of the FNE just anterior to the notochord was identified as the prechordal plate.

Vital dye mapping of the notochord and FNE on the involuting and extending ARF

Although it is difficult to identify the exact location of the prospective prechordal plate on the fate map of the early gastrula DMZ, Hama (1978) indicated that in *Cynops* it is the narrow border region between the UDMZ and LDMZ. However, the position of the prospective prechordal plate on the involuting ARF has certainly not been examined in detail, so we performed vital dye mapping to define the movement and location of the progeny of the LDMZ and UDMZ on the involuting and extending ARF. The UDMZ and LDMZ were separately stained with dye, and the vegetal (future anterior) and animal (future posterior) margins of the dye mark were tracked during gastrulation (Fig. 3). When the UDMZ was stained, the vegetal margin of the dye mark progressively elongated and involuted through the blastopore, and at the end of gastrulation (stage 13c) the posterior notochordal half of the ARF was stained. However, when the LDMZ was stained, the dye marks involuted during the early to mid gastrula stages and finally occupied the FNE.

These results show that the ARF of *Cynops* is entirely derived from surface DMZ cells, and that progeny cells of the LDMZ and UDMZ maintain their integrity during gastrulation. As shown in Fig. 2, the part of the FNE just anterior to the notochord can be identified as the prechordal plate. Combining the results of our immunohistochemical observations and vital dye mapping, we conclude that the prospective prechordal plate is located in the intermediate region between the FNE and prospective notochord during gastrulation.

Regional inductive activity of the ARF

The ARF of the late gastrula embryo (stage 13c; Figs. 1A, C) was isolated and divided into six parts (I–VI, Fig. 4A) of the same size. The inductive activity of each part was then analyzed using sandwich culture. The tissue differentiation pattern of each sandwich explant was histologically examined, and the regional identity of the induced neural structures was also analyzed by RT-PCR.

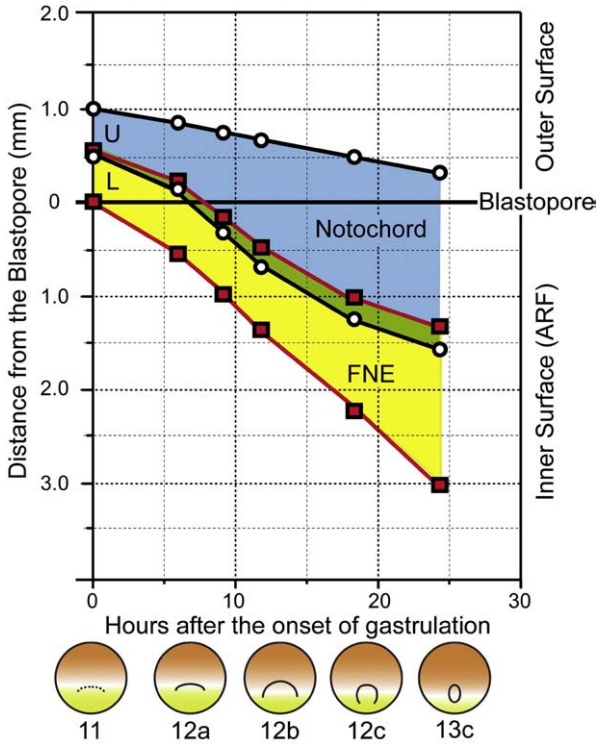

Fig. 3. Vital dye mapping of the involuting and extending archenteron roof. The upper (U) and lower (L) dorsal marginal zones (UDMZ and LDMZ, respectively) were separately stained with dye, and the position of the vegetal (future anterior) and animal (future posterior) margins of the dye was tracked during gastrulation. Results for the UDMZ and LDMZ were overlaid and the boundary between the LDMZ (red square with red line) and UDMZ (open circle with black line) was estimated. At stages 12a to 12b, the progeny of the LDMZ underlie the progeny of the UDMZ. At the late gastrula stage (stage 13c), progeny of the UDMZ occupy the posterior half of the ARF containing the prospective notochord, and the progeny of the LDMZ occupy the anterior FNE half. The border between the FNE and prospective notochord (green belt) is near the center of the ARF during gastrulation.

As shown in Fig. 4B and Table 1, none of the neural and mesodermal structures was induced by parts I and II. Part III explants had a poorly organized head structure in only 1/8 (13%). These observations indicate that almost all of the FNE does not have inductive ability. On the other hand, the posterior half of the ARF showed definite inductive activity. Neural structures were induced in 7/8 (88%) explants of part IV. Of these, 3/8 (38%) explants showed head neural structures without a notochord or with very small notochord, and 4/8 (50%) explants showed head and trunk–tail neural structures associated with a well-developed notochord and somites. The head structures were decreased in part V explants, but elongated typical trunk–tail structures were induced in all part VI explants (Table 1). A mass of endoderm was observed in all explants of parts I–III and in 50% of part IV explants, but none in parts V and VI explants. Cell lineage analysis clearly showed that parts I–III of the ARF developed into a mass of endoderm or pharyngeal endoderm (Fig. 4B), a mass of endoderm and notochord in part IV, and notochord in the posterior V and VI parts. In addition, it was clear that abundant somites were also induced by parts V and VI of the ARF; all neural structures and somites in these explants were induced by the ARF (Fig. 4B).

To confirm the regional identity of the induced neural tissues, total RNA was isolated from individual explants and RT-PCR was performed (Table 2, Fig. 4C). When explants of the anterior parts I–III were analyzed, expression of neural and somite marker genes was not detected. Neural-specific *NCAM* expression was induced in explants of parts IV–VI. Region-specific neural markers, *Otx2*, *en-2* and *Pax6*, demonstrated expression in part IV and V explants. The part VI explant

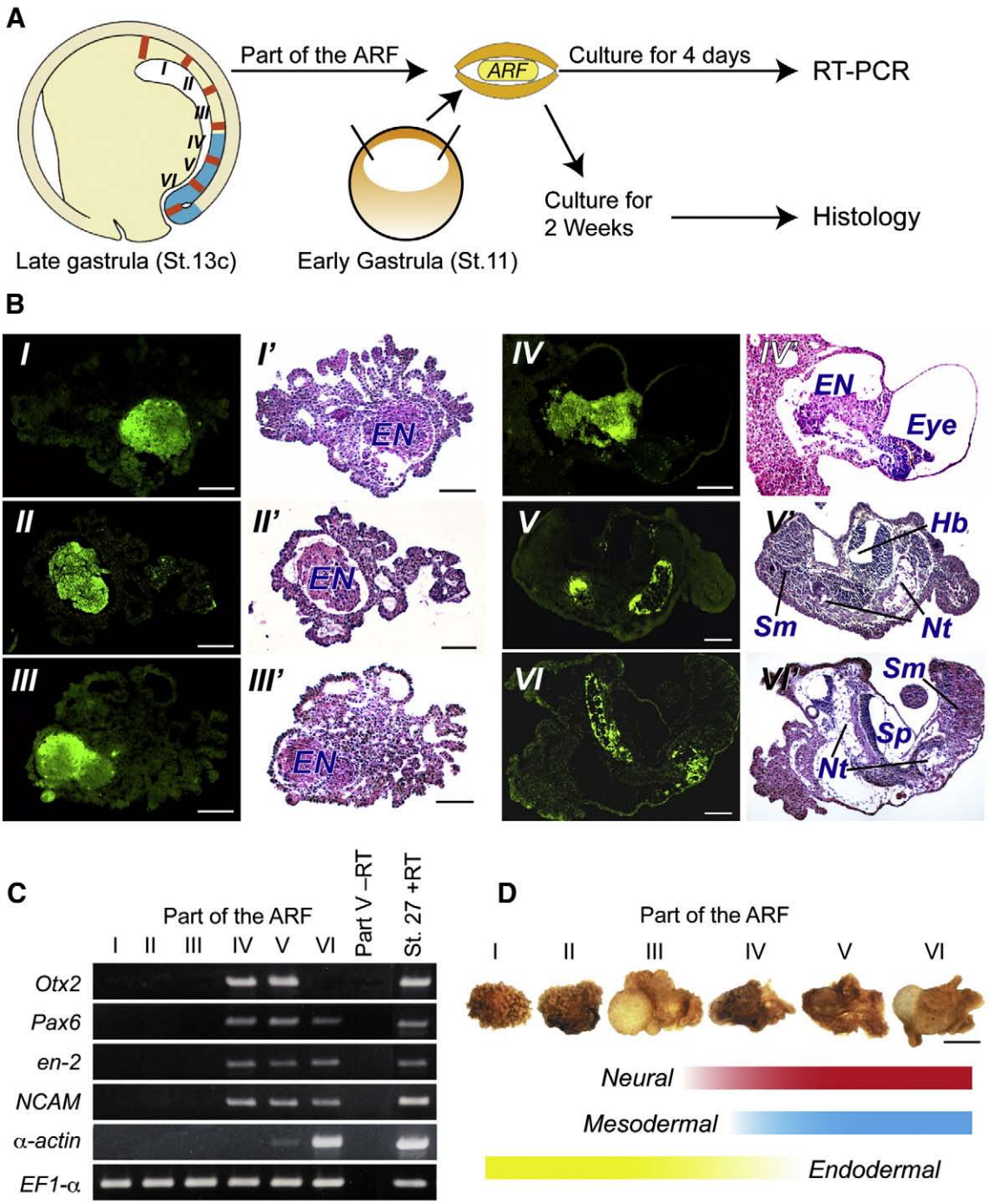

Fig. 4. Regional inductive activity of the late gastrula archenteron roof. (A) The ARF of the stage 13c late gastrula (length of ARF, approximately 3 mm) was isolated and divided into six parts of the same size. Each part was then sandwiched with two sheets of animal cap ectoderm and cultured for 4 days for RT-PCR or 2 weeks for histology. (B) The ARF was isolated as in (A) from FDA-labeled embryos and assayed by sandwich culture. Lineage of the ARF (parts I–VI) and tissue differentiation (parts I′–VI′) were analyzed. Parts I–III do not show inductive activity, but neural and mesodermal differentiation was induced by parts IV–VI. Parts V and VI of the ARF induce both neural tissues and somites. EN, mass of endoderm; Hb, hindbrain; Sp, spinal cord; Nt, notochord; Sm, somites. Bars indicate 100 μm. (C) RT-PCR analysis of the sandwich explants. Total RNA was isolated from individual sandwich explants and the expressions of *Otx2*, *en-2*, *Pax6*, neural-specific *NCAM* and *α-actin* were analyzed. *EF1-α* was used as the standard. Part V − RT and stage 27-tailbud embryos + RT were used as the negative and positive controls, respectively. (D) Shape of the sandwich explants and tissue differentiation patterns. The anterior half of the ARF self-differentiated into a mass of endodermal cells but the posterior half became notochord. Neural inducing activity is distributed in the middle to posterior half of the ARF. Bars indicate 0.5 mm.

expressed *en-2* and *Pax6*, but not *Otx2*. *α-actin* was not induced in part IV, but its expression was induced in parts V and VI (Fig. 4C). The results of RT-PCR substantiated the histological observations.

The results of sandwich culture, cell lineage analysis and RT-PCR clearly demonstrated that the ARF has two distinct domains according to their inductive activities and autonomy for tissue differentiation (Fig. 4D). The FNE (parts I–III) has autonomy for endodermal tissues and no inductive activity, whereas the posterior half of the ARF has neural inducing activity. Part IV self-differentiates mainly into endodermal tissue and tends to induce anterior neural structures. The posterior two-thirds (parts V and VI) self-differentiate into the notochord and induce mainly the trunk–tail neural structures. In

Table 1
Anterior–posterior regional inducing activity of the archenteron roof of the late gastrula of *Cynops pyrrhogaster*.

Tissue differentiation	Part of the ARF ($n=8$)[a]					
	No. (%)					
	I	II	III	IV	V	VI
Forebrain	0	0	1 (13)	7 (88)	3 (38)	1 (13)
Hindbrain	0	0	1 (13)	4 (50)	4 (50)	6 (75)
Spinal cord	0	0	0	3 (38)	7 (88)	8 (100)
Notochord	0	0	0	5 (63)[b]	7 (88)	8 (100)
Somites	0	0	0	3 (38)	7 (88)	8 (100)
Endoderm[c]	8 (100)	8 (100)	8 (100)	4 (50)	0	0
Neural differentiation pattern						
Head	0	0	1 (13)	3 (38)	1 (13)	0
Head + trunk + tail	0	0	0	4 (50)	3 (38)	1 (13)
Trunk + tail	0	0	0	0	4 (50)	7 (87)

Neural differentiation patterns: Head, forebrain/midbrain neural structures associated with eyes (including tapetum) or nose are organized; sometimes a poorly differentiated small notochord was associated with head neural structures; Trunk + tail, hindbrain/spinal cord associated with ear vesicles and well-differentiated notochord and somites are organized.

[a] Assay performed in 8 embryos. The archenteron roof (ARF) of each embryo was divided into six pieces and the organizing activity of each piece was analyzed by sandwich assay. Of these, four embryos were FDA-labeled to trace the cell lineage of the ARF.

[b] 3 of 5 have a very small notochord.

[c] Endodermal cell mass or pharyngeal endoderm.

addition to their neural inducing activity, parts V and VI have somite inducing activity.

Spatial and temporal expression patterns of Cygsc and Cybra during gastrulation

The spatial and temporal expression patterns of the *Cygsc* and *Cybra* during gastrulation were observed (Fig. 5). At the early gastrula stage, there was crescent-shaped expression of *Cygsc* (Fig. 5A) and sections showed that it was expressed in the superficial and inner cells of the LDMZ, restricted to the suprablastoporal region and not extending below it (Fig. 5F). In the early to mid gastrula, *Cygsc*-expressing cells completely involuted (Figs. 5B, G, H) and lay under the surface uninvoluted *Cybra*-expressing cells (Figs. 5L, Q, R). In the mid to late gastrula, *Cygsc* expression was progressively restricted to the middle region of the ARF (Fig. 5C), and then to the intermediate region between the FNE and notochord (Fig. 5D). Sections of stage 13c late gastrula shows that *Cygsc* is expressed mainly in the middle portion of the ARF (parts III and IV of Fig. 4A) and expression decreased in both the anterior and posterior directions (Fig. 5I). Finally, *Cygsc* expression was restricted to the FNE just anterior to the notochord, beneath the forebrain part of the neural plate (Figs. 5E, J). In *Xenopus*, *gsc* is expressed in the deep layer of the dorsal lip of the blastopore, which is fated to become pharyngeal endoderm, prechordal plate and notochord, and this expression is extended to the leading edge of the endoderm. During gastrulation, *gsc* expression is confined to the prechordal plate and anterior endoderm region of the ARF (Cho et al., 1991; De Robertis, 2004). *Cygsc* expression in the early gastrula DMZ in *Cynops* is confined to the surface LDMZ region, and the expression pattern is different to that of *Xenopus gsc* due to the differences in germ layer structure, however, the present *Cygsc* expression pattern during gastrulation is essentially the same as in *Xenopus*.

In *Xenopus*, ring-shaped *Xbra* expression is identified in the mesodermal marginal zone of the pre-gastrula embryo (Smith et al., 1991; Vodicka and Gerhart, 1995). However, as shown in Figs. 5K and P, *Cybra* was not expressed in any region of the embryo in the early gastrula stage, as previously reported (Sone et al., 1997; Doi et al., 2000). At the mid gastrula stage, *Cybra* expression was first detected as a crescent-shaped area in the upper blastopore (Fig. 5L), the area corresponding to the progeny of the UDMZ that were fated to the notochord, as indicated by vital dye mapping (Fig. 3). Sections also showed that *Cybra* expression was restricted to the uninvoluted dorsal lip, which was underlined by involuted *Cygsc*-expressing FNE (Figs. 5L, Q, R). *Cybra* expression became more prominent as gastrulation proceeded. At the late gastrula stage, ring-shaped *Cybra* expression was observed around the yolk plug on the egg surface (Fig. 5M). Sections reveal that *Cybra* expression is mainly located in the posterior one-third (parts V and VI, Fig. 4A) and expression decreased in part IV (Fig. 4A) of the ARF (Fig. 5S). *Cybra* expression pattern at late gastrula is essentially the same as in *A. mexicanum* (Johnson et al., 2003). In the early neurula, *Cybra* expression was restricted to the involuted notochord and the uninvoluted part of the slit blastopore (Fig. 5N). Finally, *Cybra* expression was preferentially restricted to the notochord in the neurula stage (Figs. 5O, T). At this stage, the anterior border of the *Cybra*-expressing ARF coincided with the anterior tip of the neural groove.

Although it was unclear whether the anterior tip of the *Cybra*-expressing region overlapped with *Cygsc* expression in the late gastrula stage, we concluded that the *Cybra*-expressing ARF coincided with the prospective notochord as revealed by vital dye mapping (Fig. 3) and cyNot-2 (Fig. 2). Thus, the anterior FNE and posterior prospective notochord domains of the ARF were identified as the *Cygsc*- and *Cybra*-expressing domains, respectively.

Cygsc-expressing domain in the Keller sandwiches planarly induced Cybra-expressing cells

As shown in Fig. 5, *Cybra* expression was induced in the progeny cells of the UDMZ during the early to mid gastrula stages. We previously demonstrated that the LDMZ has potent notochord inducing activity (Kaneda, 1981; Kaneda et al., 2002; Sakaguchi et al., 2002), and suggested that the LDMZ induces notochord in the neighboring UDMZ by a planar (tangential) interaction (Kaneda, 1981). To determine the mode of interaction between the LDMZ and UDMZ, the DMZ of the early gastrula was isolated and cultured in Keller sandwiches (Doniach, et al., 1992; Doniach, 1993; Poznanski et al., 1997).

As a control, UDMZ or LDMZ was isolated and cultured alone for 1 or 24 h (Fig. 6A) and then hybridized with *Cygsc* or *Cybra* probe, respectively. All 1 and 24 h LDMZ expressed *Cygsc* (Figs. 6E, F) but not *Cybra* (Figs. 6I, J). *Cybra* and *Cygsc* expression was also analyzed in the isolated UDMZ. *Cygsc* expression was observed in 18% (2 / 11, Fig. 6C) and 21% (4 / 19, Fig. 6D) of the 1 and 24 h UDMZ. *Cybra* expression was not detected in the 1 h UDMZ (Fig. 6G) but weak *Cybra* expression was identified in 26% (5 / 19, Fig. 6H) of the 24 h UDMZ. As shown in Figs. 5A and F, *Cygsc* expression in the early gastrula DMZ gradually decreased from blastopore (pigment line) to the upper UDMZ, it is difficult to isolate the UDMZ without contamination of the lower *Cygsc*-expressing LDMZ cells. Indeed, *Cygsc* expression was observed in 18 and 21% of the 1 and 24 h UDMZ, and *Cygsc*-expressing

Table 2
Expression of marker genes in the sandwich explants of each part of the archenteron roof.

Marker genes	Part of the ARF ($n=7$)					
	No. (%)					
	I	II	III	IV	V	VI
Otx2	0	0	1 (14)	6 (86)	5 (71)	1 (14)
en-2	0	0	1 (14)	6 (86)	7 (100)	7 (100)
Pax6	0	0	1 (14)	6 (86)	7 (100)	7 (100)
NCAM	0	0	1 (14)	6 (86)	7 (100)	7 (100)
α-actin	0	0	0	1 (14)	5 (71)	7 (100)

The archenteron roof (ARF) of seven individual embryos was dissected and divided into six parts from which sandwich explants were made. After cultivation for 4 days, total RNA was isolated from each explant and assayed by RT-PCR.

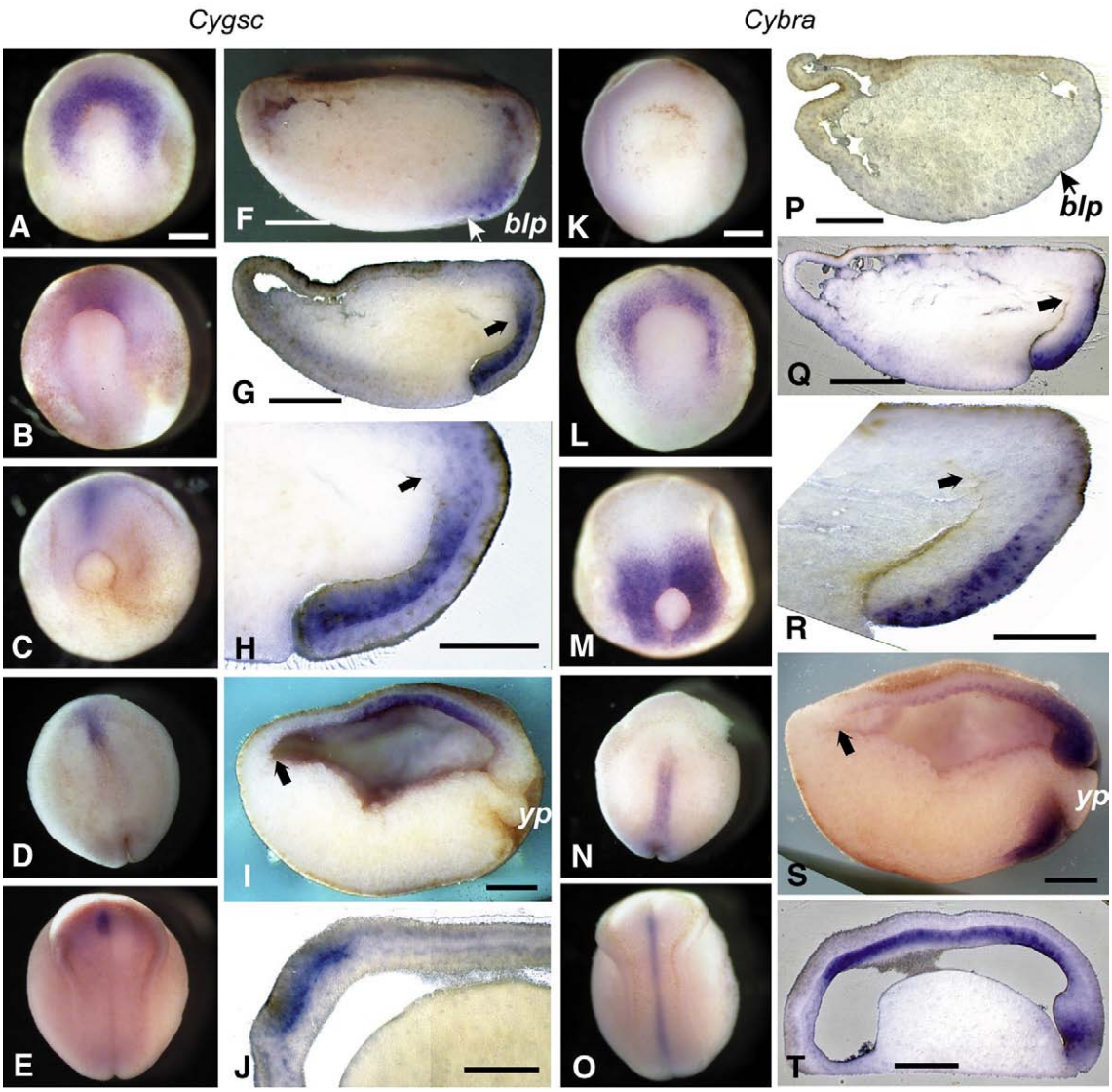

Fig. 5. Spatial and temporal expression patterns of *Cybra* and *Cygsc*. *Cygsc* (A–J) and *Cybra* (K–T) expression patterns during gastrulation were observed by *in situ* hybridization. *Cygsc* expression can be seen in the suprablastoporal endoderm (LDMZ) region of the stage 11 early gastrula (A, F). At the mid gastrula stage (stage 12b), *Cygsc*-expressing cells involute and underlie the surface *Cybra*-expressing region (B, G, H). At the late gastrula stage (stage 13c), *Cygsc* expression is progressively restricted to the anterior part of the prospective notochord and the posterior part of the FNE (C, I). From the early neurula stage (D, stage 15) onward, expression is further restricted to the ARF underlying the anterior neural fold region of the neural plate (E, J, stage 18). In the stage 11 early gastrula, *Cybra* expression was not detected in any part of the embryo (K, P). At the mid gastrula stage (stage 12b), *Cybra* expression was first detected in the outer suprablastoporal dorsal lip region (L, Q, R). *Cybra*-expressing cells involuted and at the late gastrula stage (stage 13c) there is ring-shaped *Cybra* expression around the yolk plug (M). Sections indicate that *Cybra* was mainly expressed at the posterior one-third of the ARF (S). At the early neurula stage (stage 15), *Cybra* is expressed in the middle to posterior part of the ARF and in the dorsal lip region around the slit blastopore (N). In the neurula (stage 18), *Cybra* expression is restricted to the notochord. The anterior tip of the *Cybra*-expressing notochord coincides with the anterior tip of the neural groove (O, T). Arrows in G, H, Q, R and S indicate anterior margin of the involuting ARF. In all figures, left and right represent the anterior and posterior directions, respectively. Blp: blastopore; yp: yolk plug. Bars indicate 0.5 mm.

LDMZ cells have potent notochord inducing activity, *Cybra* expression observed in the 24 h UDMZ (Fig. 6H) may be due to contamination by *Cygsc*-expressing LDMZ cells in the UDMZ isolates. These results indicate that *Cybra*-expressing cells have not yet been induced in the UDMZ at the early gastrula stage.

In the Keller sandwiches (Fig. 6B), *Cybra* and *Cygsc* expression was analyzed after cultivation for 1 or 24 h (Figs. 6K–N). After 1 h cultivation, *Cygsc* expression was identified at the tip of the explants (Fig. 6K), but *Cybra* expression was not (Fig. 6M). During cultivation, the explants elongated and at 24 h, *Cygsc* expression was maintained at the anterior tips of the explants (Fig. 6L). *Cybra* expression was not identified in the 1 h explants, but was induced in the central, elongated portion of the 24 h explants (Fig. 6N). Because no signs of involution were observed in the Keller sandwiches, these results indicated that the *Cygsc*-expressing LDMZ planarly induced *Cybra*-expressing notochord in the UDMZ.

Discussion

Two distinct domains of the involuting and extending ARF

The ARF of *Xenopus* embryos consists of two layers, roof-endoderm and mesoderm, but the surface LDMZ and UDMZ of the *Cynops* early gastrula involuted as a continuous sheet and formed a monolayered ARF, except at its most anterior end (Fig. 1). Although no histological differences were observed throughout the ARF, immunohistochemical observations and the sandwich assay revealed that the gastrula ARF is clearly divided into a posterior prospective notochord and anterior FNE (Figs. 2 and 4). Vital dye mapping (Fig. 3) showed that the progeny cells of the uninvoluted LDMZ and UDMZ form the FNE and prospective notochord domains, respectively. These results also indicate that the boundary between the FNE and prospective notochord is located at the center of the ARF during gastrulation.

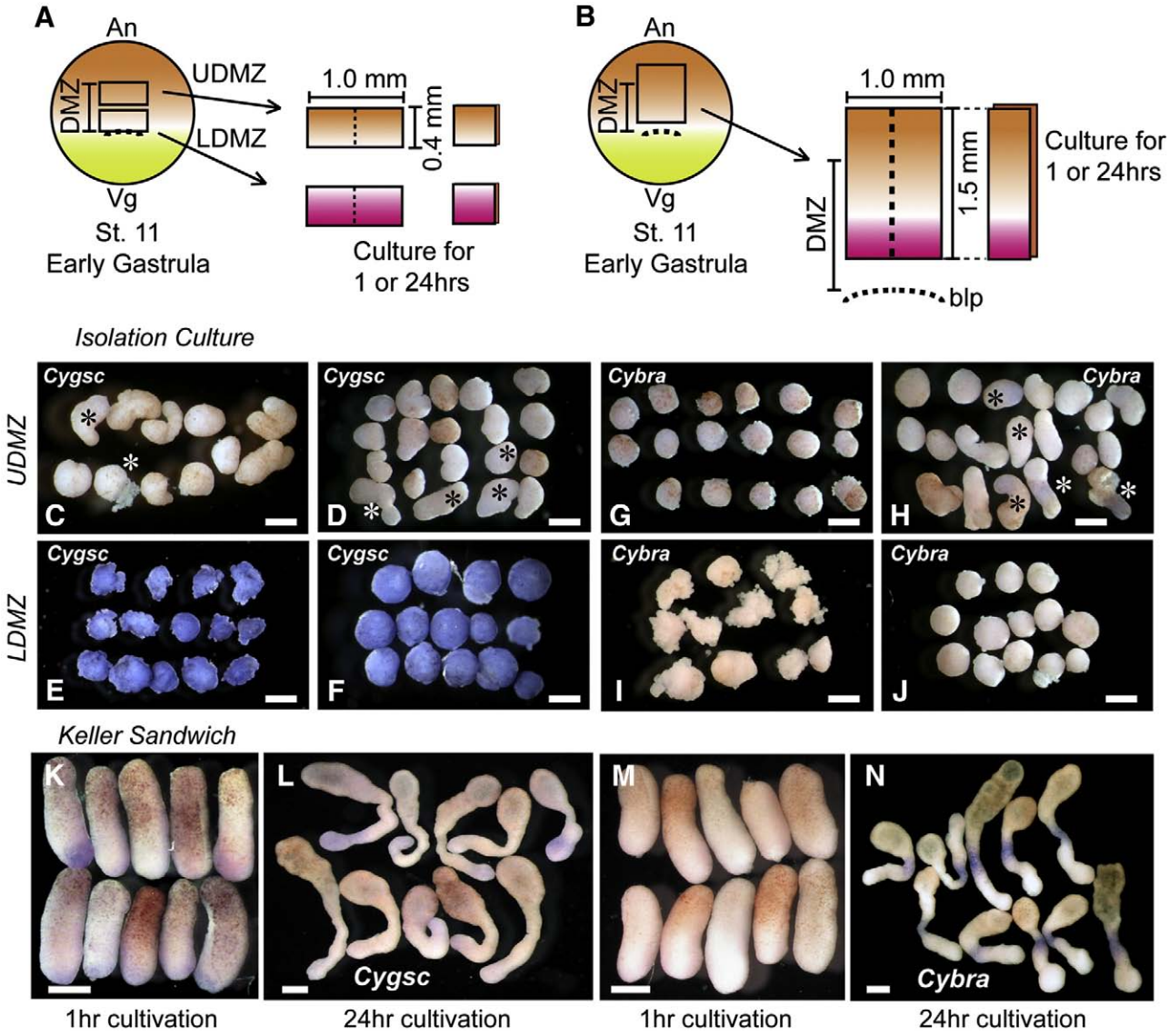

Fig. 6. *Cybra* gene expression is planarly induced in Keller sandwiches of early gastrula dorsal marginal zone. (A) LDMZ and UDMZ of the early gastrula (stage 11) were isolated and cultured alone for 1 or 24 h and then hybridized with *Cygsc* (C–F) or *Cybra* (G–J) probe. (B) Experimental procedures of Keller sandwiches. The DMZ of the stage 11 gastrulae was dissected and cultured in Keller sandwiches for 1 or 24 h and then hybridized with *CyGsc* (K, L) or *CyBra* (M, N) probe. To eliminate contamination of the bottle cells, the vegetal (future anterior) margin was in the middle portion of the lower DMZ and the animal (future posterior) margin was in the presumptive posterior neural plate. An: Animal; Vg: vegetal; blp: blastopore (pigment line). In the case of isolation culture (C–J), *Cygsc* expression was identified in all 1 and 24 h LDMZ isolates (E, F). *Cygsc* expression was also identified in some isolates in 1 h (2/11, C) or 24 h (4/19, D) UDMZ (marked by asterisk). *Cybra* expression was examined in LDMZ (I, J) and UDMZ (G, H) isolates. *Cybra* expression was not observed in 1 and 24 h LDMZ (I, J) and 1 h UDMZ (G). *Cybra* expression was detected in some 24 h UDMZ isolates (marked by asterisk, 5/19, H). In the case of Keller sandwiches (K–N), *Cygsc* expression can be seen in the anterior tip region of the explants (K, L). *Cybra* expression was not detected in 1 h explants (M), but was induced in the middle elongated part of the explants (N). Bars indicate 0.5 mm.

Notochord induction in Cynops occur at the first half of gastrulation

Although spatial localization varies according to the defining criteria used, it has been shown that the DMZ of the late blastula to early gastrula of *Xenopus* comprises multiple domains with different prospective fates, functions and gene expression patterns. Of these, at least two major domains have been identified in the dorsal side of the pre-gastrula stage *Xenopus*: the sub-blastoporal Nieuwkoop center and the suprablastoporal organizer. Although it has been reported that the Nieuwkoop center and the organizer share the same region or the same molecular components (Kimelman et al. 1992; Vonica and Gumbiner, 2007), the Nieuwkoop center is defined as a part that retains its endodermal fate, but induces an organizer containing notochord and somites (Gimlich and Gerhart, 1984; Gerhart et al., 1991). Although the locations of these centers, and their spatial and temporal functions, have not been fully elucidated, the *gsc*-expressing and *Xbra*-expressing subdomains were established in the organizer region by the interactions between and within these centers before the onset of gastrulation in *Xenopus* (see reviews, Harland and Gerhart, 1997; Gerhart, 2001).

As shown in Fig. 5, our results demonstrated that in *Cynops*, *Cygsc* is expressed in the LDMZ from the onset of gastrulation, whereas *Cybra* expression only begins in the mid gastrula stage. We have previously shown that the LDMZ has autonomy for endodermal differentiation, while it has potent notochord inducing activity. When the LDMZ was combined with presumptive ectoderm, *Cybra* expression was induced as a result of notochord cell induction by the LDMZ (Kaneda et al., 2002). The LDMZ lost its notochord inducing activity soon after involution (Kaneda, 1980) or *in vitro* cultivation (Suzuki et al., 1984; Kaneda et al., 2002). In addition to *Cygsc*, the LDMZ has been shown to express the *Cynops* homologs of *chordin*, *lim-1* and *noggin*, but not *Cybra*, and these gene expressions are maintained in isolated

and *in vitro* cultured LDMZ (Yokota et al., 1998; Kaneda et al., 2002). Furthermore, it has been demonstrated that the LDMZ alone can induce a complete secondary axis due to its notochord inducing activity (Yamamoto and Suzuki, 1994; Imoh et al., 1998), and that the secondary axis inducing activity is restricted to the suprablastoporal region of an area 30° from the blastopore along the animal–vegetal axis and 60° laterally (Yamamoto and Suzuki, 1994), an area identical to the *Cygsc*-expressing LDMZ (Fig. 5A). Although we only investigated the *Cygsc* and *Cybra* expression patterns, these results strongly indicate that the *Cynops* LDMZ has similar properties to the *Xenopus* Nieuwkoop center in its self-differentiation, organizing activity and gene expressions, as previously reported (Sakaguchi et al., 2002).

As shown in Figs. 5K and P, *Cybra* was not expressed in any part of the early gastrula, as previously reported (Sone et al., 1997; Doi et al., 2000). In *Xenopus*, *Xbra* expression is an immediate early response to mesoderm induction, and *Xbra* is expressed in the mesodermal marginal zone of the pre-gastrula embryo, followed by localization to the blastopore, notochord and somites (Smith et al., 1991; Vodicka and Gerhart, 1995; Kumano et al. 2001). However, in the present study, *Cybra* expression was first observed around the outer surface of the dorsal lip of the mid gastrula, and thereafter its expression was confined to the entire notochord (Figs. 5K–T). This *Cybra* expression pattern is significantly different from that of *Xenopus* and other anurans (Pollet et al., 2005; del Pino et al., 2007), demonstrating that notochord and mesoderm induction in *Cynops* occurs during gastrulation.

As mentioned earlier, the notochord inducing activity of the LDMZ disappeared soon after involution. In the mid gastrula (stage 12c) when the involuted *Cygsc*-expressing LDMZ underlaid the surface UDMZ (Fig. 5H), the surface UDMZ has already been induced to express *Cybra* (Fig. 5R). It has been reported that the upper one-third of the early gastrula DMZ is not yet mesodermized, and self-differentiates into atypical epidermis (Kaneda and Hama, 1979). When the upper one-third of the early gastrula DMZ was replaced with animal cap ectoderm, it was induced to become notochord until the stage 12c mid gastrula (Kaneda, 1981). We therefore expected *Cygsc*-expressing LDMZ to planarly induce *Cybra*-expressing notochord in the uninvoluted UDMZ, and our results with Keller sandwiches show that the LDMZ planarly induces *Cybra* expression in the neighboring UDMZ (Figs. 6M, N). As indicated by Doniach et al. (1992), Doniach (1993) and Poznanski et al. (1997), it is difficult to exclude the possibility that the UDMZ has already presented the notochord inducing signals before the onset of gastrulation, even when *Cybra* expression was not detected at that stage. As a control, however, when the UDMZ are isolated and cultured alone, *Cybra* expression was not autonomously induced in these isolates (Figs. 6G, H). These results indicate that the *Cygsc*-expressing LDMZ planarly induces the *Cybra*-expressing notochord during early to mid gastrula stages. In addition, as shown in Figs. 6L and N, the middle *Cybra*-expressing regions of the Keller sandwiches showed convergent-extension movement, and became considerably elongated. In normal gastrulation, the prospective notochord exhibits convergent extension through planar cell polarity (PCP) (Keller, 2002; Ninomiya et al., 2004; Shook and Keller, 2008). It is therefore possible that in the Keller sandwiches, PCP related genes were also induced by the LDMZ.

Comparing the present results with those for *Xenopus*, *Xenopus* undergoes notochord (dorsal mesoderm) induction prior to the onset of involution. Internal gastrulation (Nieuwkoop and Florschütz, 1950; Keller, 1976) and vegetal rotation (Winklbauer and Schürfeld, 1999) facilitate intra-DMZ interactions between the inner and outer DMZ and upper and lower DMZ. *Gsc*-expressing and *Xbra*-expressing domains are established by these intra-DMZ interactions prior to the onset of involution. Thus, the regional specificities of the future ARF are pre-patterned on the DMZ. On the other hand, *Cynops* undergoes these interactions during the early to mid gastrula stages, and regional specificity of the ARF was established at the mid gastrula stage. In this sense, it is likely that the *Xenopus* early gastrula that begins involution is equivalent to the *Cynops* mid gastrula. The first half of *Cynops* gastrulation can therefore be designated the notochord induction phase (Fig. 7).

Organizing activity of the ARF is restricted to the prospective notochord domain and the second half of Cynops gastrulation is specified as neural induction phase

Although their stage criteria and positioning of the ARF differed from the present study, Okada and Hama (1945) and Suzuki et al. (1975) investigated regional differences in inductive activity of the involuting and extending ARF of *Cynops*. Dividing the ARF into several parts, they showed that the anterior one-third (Suzuki et al., 1975) or anterior half (Okada and Hama, 1945) of the mid to late gastrula ARF has no neural inducing activity. Suzuki et al. (1975) also demonstrated that the prospective neural ectoderm in contact with the posterior two-thirds of the ARF gradually neuralized from posterior to anterior to self-differentiate into neural identities. The same situation was also reported in *Xenopus*, in which *Xotx2* expression travels through the prospective neuroectoderm with movement of the underlying ARF (Blitz and Cho, 1995).

As shown in Fig. 4 and Tables 1 and 2, we determined the prospective fate, self-differentiation and organizing activity of the ARF, finding that the FNE lost its inductive activity, and the posterior prospective notochord half of the ARF that had been induced to become notochord in turn acquired neural inducing activity from the mid gastrula stage onward. Our results also indicate that contact between the induced notochord and the overlying prospective neuroectoderm occurs from the mid gastrula stage onward (Fig. 3). As shown in Tables 1 and 2, the prospective notochord induces neural tissue of a somewhat broader regional character than would be expected from its final position in the embryo. The anterior end of the prospective notochord (part IV) tended to induce forebrain structures, whereas the posterior end of the prospective notochord (part VI) tended to induce trunk–tail structures. The intermediate part V induced both forebrain and trunk–tail neural structures. Our RT-PCR results support the histological findings that part IV induces *Otx2*, *Pax6* and *en-2*, but not α-*actin*. Part VI did not induce *Otx2*, but α-*actin* was induced in these explants, and part V induced both *Otx2* and α-*actin* (Fig. 4C, Table 2). These results demonstrate that forebrain inducing activity is not restricted to a specific region, but is distributed to a broad region of prospective notochord, even at the late gastrula stage. These results strongly indicate that neural induction is initiated in the mid gastrula, and that the second half of *Cynops* gastrulation can be designated the neural induction phase.

Comparing the present results with those for *Xenopus*, notochord formation and the regional specification of the future ARF has been established in the early gastrula DMZ before the onset of gastrulation. Thus we propose that *Xenopus* gastrulation be specified as a process to realize neural patterning by the interaction between the already patterned ARF and the overlaying ectoderm. On the other hand, the urodele embryo undergoes two temporally distinct steps of gastrulation: notochord induction and regional specification of the ARF in the first half, and anteroposterior neural patterning in the second half of gastrulation (Fig. 7).

Origin of the prechordal plate and patterning of the anteroposterior regional specificity of the neural tissues

The prechordal plate was recently defined as the tissue located at the rostral end of the notochord that expresses prechordal plate marker genes such as *gsc* and *lim-1* (Garcia-Martinez et al., 1997; Latinkic and Smith, 1999; Kazanskaya et al., 2000; Kiecker and Niehrs, 2001; Chapman et al., 2002, 2003). Because it is difficult to determine the precise location of the prechordal plate, or to distinguish precisely

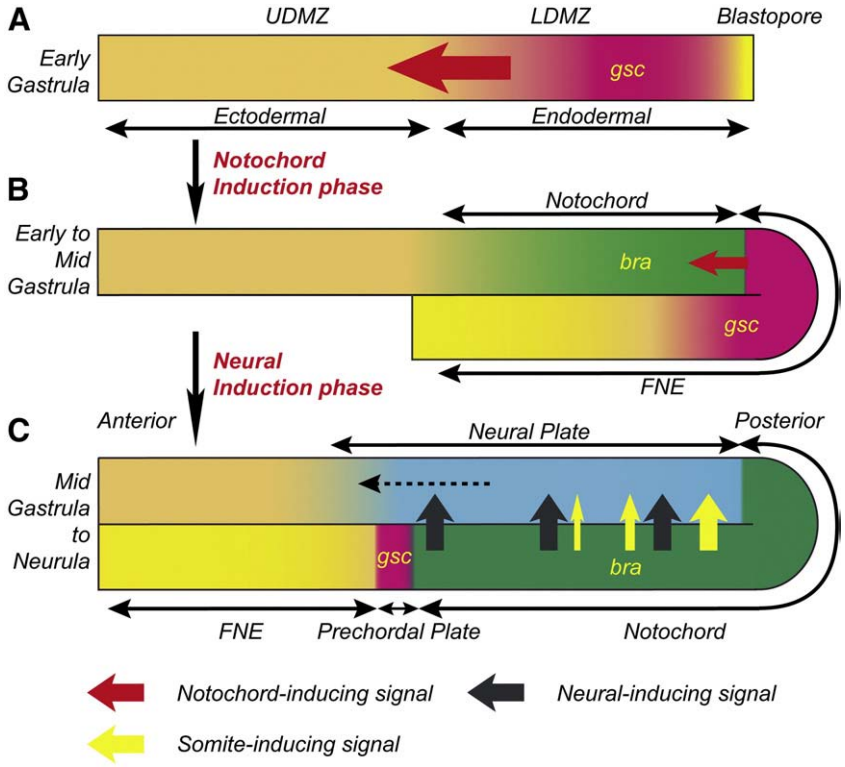

Fig. 7. Spatial and temporal process of anteroposterior regional patterning of the involuted and extending archenteron roof. (A) At the early gastrula stage, the suprablastoporal region expressing *Cygsc* is identified as the "prechordal region" and the notochord is not yet induced. (B) During early to mid gastrulation, the prechordal region planarly induces *Cybra*-expressing notochord. (C) As involution proceeds, the prechordal region forms the fore-notochordal endodermal roof (FNE) and *Cygsc* expression is progressively restricted to the FNE just anterior to the induced notochord, forming the prechordal plate. The entire notochord emanates an "activating" neural inducing signal to induce the neural plate in the overlaying prospective neuroectoderm. The induced neural cells will homeogenetically induce neural cells to establish the final pattern of the neural plate (dashed black arrow). The posterior part of the notochord emanates not only the neural inducing signal, but also a somite (lateral mesoderm) inducing signal, which will act as a "transformation" signal. In this figure, anterior is represented as left.

the limit between the prechordal plate and notochord on the involuting and extending ARF, Foley et al. (1997) used the term "prechordal region" instead of prechordal plate and reported that the avian prechordal region does not have neural inducing activity, but does maintain anterior neural identities. As shown in Fig. 5, *Cygsc*-expressing cells completely involuted at the mid gastrula stage and formed the FNE. In the late gastrula to neurula stage, *Cygsc* expression was spatially and temporarily restricted to the middle portion of the ARF (parts III and IV, Fig. 5I) and then to the prechordal plate part of the FNE, just anterior to the notochord and underlying the forebrain part of the neural plate (Figs. 5D, E, J). Finally, *Cygsc*-expressing cells were confined to the prechordal plate. Thus, it is possible that the LDMZ, which forms the FNE, corresponds to the prechordal region. The main function of the prechordal region is to planarly induce the notochord at the early to mid gastrula stages (Figs. 7A, B). As involution proceeds, the notochord inducing activity of the prechordal region disappears, and finally the region survives as the prechordal plate (Figs. 7B, C). It was unclear from our experiments whether the prechordal plate retained neural inducing activity. We previously demonstrated that isolated and *in vitro* cultured LDMZ lose their notochord inducing activity, while retaining weak but definite neural inducing activity (Kaneda et al., 2002). The neural inducing activity of the LDMZ almost completely disappears with prolonged cultivation *in vitro* (Suzuki et al., 1984). In *Xenopus*, *gsc*-expressing cells involute and form the prechordal plate and anterior endoderm, and the prechordal plate acts as a source for head-organizing activity (Cho et al., 1991; Gerhart, 2001; Kiecker and Niehrs, 2001; De Robertis, 2004). As shown in Fig. 5 and Tables 1 and 2, the *Cygsc*-expressing ARF was gradually restricted to the junctional region between the FNE and prospective notochord, and the neural inducing activity of the ARF shifted to the middle to posterior part of the ARF. These observations indicate that neural inducing activity of *Cygsc*-expressing cells is transiently maintained during normal gastrulation, but is lost in the late gastrula, at which stage the main cellular source of neural inducing signals shifts to the induced notochord.

The prospective notochord expresses *Cybra* (Fig. 5S) and exhibits trunk–tail organizing activity: it induces both neural structures and somites and organized typical trunk–tail structures (Fig. 4). On the other hand, although the anterior part of the prospective notochord tends to induce forebrain, head inducing activity is distributed to a broad region of prospective notochord. It has been suggested that the regional neural identities of the neural plate are affected by the surrounding mesoderm, such as notochord and somites (reviewed by Takaya, 1978), and it was recently shown that caudalizing signals from somites posteriorize the forebrain neural structures (Muhr et al., 1997; Gould et al., 1998; Wacker et al., 2004, Wilson and Maden, 2005). Therefore, it is possible that head-organizing activity, or Nieuwkoop's activation signal, is the neural inducing activity that emanates not from a restricted part of the ARF, but from the entire notochord, and that the transformation signals are coupled with somite inducing signals (Fig. 7C). If prospective neuroectoderm cells receive only a neural inducing signal, they will form head neural structures, but if they receive both neural and somite inducing signals, they will form more posterior neural structures. The association of notochord and somites will also determine the final neural pattern.

Acknowledgment

We would like to thank Professor Emeritus Akio S. Suzuki of the Department of Biological Science, Faculty of Science, Kumamoto University, for his encouragement and kind gift of the cyNot-2 antibody.

References

Adelmann, H.B., 1932. The development of the prechordal plate and mesoderm of *Amblystoma punctatum*. J. Morph. 54, 1–67.

Blitz, I.L., Cho, W.Y., 1995. Anterior neuroectoderm is progressively induced during gastrulation: the role of the *Xenopus* homeobox gene *orthodenticle*. Development 121, 993–1004.

Chapman, S.C., Schubert, F.R., Schoenwolf, G.C., Lumsden, A., 2002. Analysis of spatial and temporal gene expression patterns in blastula and gastrula stage chick embryos. Dev. Biol. 245, 187–199.

Chapman, S.C., Schubert, F.R., Schoenwolf, G.C., Lumsden, A., 2003. Anterior identity is established in chick epiblast by hypoblast and anterior definitive endoderm. Development 130, 5091–5101.

Cho, K.W., Biumberg, B., Steinbeisser, H., De Robertis, E.M., 1991. Molecular nature of Spemann's organizer: the role of the *Xenopus* homeobox gene *goosecoid*. Cell 67, 1111–1120.

Delarue, M., Sanches, S., Johnson, K.E., Darribere, T., Boucaut, J.-C., 1992. A fate map of the superficial and deep circumblastoporal cells in the early gastrula of *Pleurodeles waltl*. Development 114, 135–146.

del Pino, E.M., Venegas-Ferrin, M., Romero-Carvajal, A., Montenegro-Larrea, P., Sáenz-Ponce, N., Moya, I.M., Alarcón, I., Sudou, N., Yamamoto, S., Taira, M., 2007. A comparative analysis of frog early development. Pro. Natl. Acad. Sci. 104, 11882–11888.

De Robertis, E.M., 2004. *Goosecoid* and gastrulation. In: Stern, C.D. (Ed.), Gastrulation, From Cells to Embryo. Cold Spring Harbor Press, Cold Spring Harbor, New Yolk, pp. 581–589.

Doi, J., Niigaki, H., Sone, K., Takabatake, T., Takeshima, K., Yasui, K., Tosuji, H., Tsukahara, J., Sakai, M., 2000. Distribution of dorsal-forming activity in pre-cleavage embryos of the Japanese newt, *Cynops pyrrhogaster*: effects of deletion of vegetal cytoplasm, UV irradiation, and lithium treatment. Dev. Biol. 223, 154–168.

Domingo, C., Keller, R., 1995. Induction of notochord cell interaction behavior and differentiation by progressive signals in the gastrula of *Xenopus laevis*. Development 121, 3311–3321.

Doniach, T., 1993. Planar and vertical induction of anteroposterior pattern during the development of the amphibian central nervous system. J. Neurobiol. 24, 1256–1275.

Doniach, T., Phillips, C.R., Gerhart, J.C., 1992. Planar induction of anteroposterior pattern in the developing central nervous system of *Xenopus laevis*. Science 257, 542–545.

Eagleson, G.W., 1996. Developmental neurobiology of the anterior areas in amphibians: urodele perspective. Int. J. Dev. Biol. 40, 735–743.

Foley, A.C., Storey, K.G., Stern, C.D., 1997. The prechordal region lacks neural inducing ability, but can confer anterior character to more posterior neuroepithelium. Development 124, 2983–2996.

Fujisaki, A., Hasegawa, H., Miyata, A., 2000. Observations of amphibian embryos by gelatin embedding methods. Iden 54, 80–82 (in Japanese).

Garcia-Martinez, V., Darnell, D.K., Lopez-Sanchez, C., Sosic, D., Olson, E.N., Schoenwolf, G.C., 1997. State of commitment of prospective neural plate and prospective medoderm in late gastrula/early neurula stages of avian embryos. Dev. Biol. 181, 102–115.

Gerhart, J.C., Doniach, T., Stewart, R., 1991. Organizing the *Xenopus* organizer. In: Keller, R., ClarkJr. Jr., W.H., Griffin, F. (Eds.), Gastrulation: Movements, Patterns and Molecules. Plenum Press, New Yolk, pp. 57–77.

Gerhart, J.C., 2001. Evolution of the organizer and the chordate body plan. Int. J. Dev. Biol. 45, 133–153.

Gimlich, R.L., Gerhart, J.C., 1984. Early cellular interactions promote embryonic axis formation in *Xenopus laevis*. Dev. Biol. 104, 117–130.

Gould, A., Itasaki, N., Krumlauf, R., 1998. Initiation of rhombomeric *Hoxb4* expression requires induction by somites and retinoid pathway. Neuron 21, 39–51.

Grunz, H., 1993. The dorsalization of Spemann's organizer takes place during gastrulation in *Xenopus laevis* embryos. Dev. Growth Differ. 35, 25–32.

Hama, T., 1978. Dynamics of the organizer. New findings on the regionality and morphogenetic movement of the organizer. In: Nakamura, O., Toivonen, S. (Eds.), Organizer—a Milestone of a Half-century from Spemann. Elsevier/North Holland Biomedical Press, pp. 71–90.

Harland, H., Gerhart, J., 1997. Formation and function of Spemann's organizer. Annu. Rev. Cell Dev. Biol. 13, 611–667.

Imoh, H., Yamamoto, Y., Terahara, T., Moody, S.A., Suzuki, A.S., 1998. Timing and mechanisms of mesodermal and neural determination revealed by secondary embryo formation in *Cynops* and *Xenopus*. Dev. Growth Differ. 40, 439–448.

Johnson, A.D., Crother, B., White, M.E., Patient, R., Bachvarova, R.F., Drum, M., Masi, T., 2003. Regulative germ cell specification in axolotl embryos: a primitive trait conserved in the mammalian lineage. Phil. Trans. R. Soc. Lond. B 358, 1371–1379.

Kaneda, T., 1980. Studies on the formation and state of determination of the trunk organizer in the newt, *Cynops pyrrhogaster*. II. Inductive effect from the underlying cranial archenteron roof. Dev. Growth Differ. 22, 841–849.

Kaneda, T., 1981. Studies on the formation and state of determination of the trunk organizer in the newt, *Cynops pyrrhogaster*. III. Tangential induction in the dorsal marginal zone. Dev. Growth Differ. 23, 553–564.

Kaneda, T., Hama, T., 1979. Studies on the formation and state of determination of the trunk organizer in the newt, *Cynops pyrrhogaster*. Roux's Arch. Dev. Biol. 187, 25–34.

Kaneda, T., Suzuki, A.S., 1983. Studies on the formation and state of determination of the trunk organizer in the newt, *Cynops pyrrhogaster*. IV. The association of neural inducing activity with the mesodermization of the trunk organizer. Roux's Arch. Dev. Biol. 192, 8–12.

Kaneda, T., Miyazaki, K., Kudo, R., Goto, K., Sakaguchi, K., Matsumoto, M., Todaka, S., Yoshinaga, K., Suzuki, A.S., 2002. Regional specification of the head and trunk-tail organizers of a urodele (*Cynops pyrrhogaster*) embryo is patterned during gastrulation. Dev. Biol. 244, 66–74.

Kazanskaya, O., Glinka, A., Niehrs, C., 2000. The role of *Xenopus dickkorf1* in prechordal plate specification and neural patterning. Development 127, 4981–4992.

Keller, R.E., 1976. Vital dye mapping of the gastrula and neurula of *Xenopus laevis*. II. Prospective areas and morphogenetic movements of the deep layer. Dev. Biol. 51, 118–137.

Keller, R., 2002. Shaping the vertebrate body plan by polarized embryonic cell movements. Science 298, 1950–1954.

Kiecker, C., Niehrs, C., 2001. The role of prechordal mesendoderm in neural patterning. Curr. Opin. Neurobiol. 11, 27–33.

Kimelman, D., Christian, J.L., Moon, R.T., 1992. Synergistic principles of development: overlapping patterning systems in *Xenopus* mesoderm induction. Development 116, 1–9.

Kumano, G., Ezal, C., Smith, W.C., 2001. Boundaries and functional domains in the animal/vegetal axis of *Xenopus* gastrula mesoderm. Dev. Biol. 236, 465–477.

Lane, M.C., Keller, R., 1997. Microtubule disruption reveals that Spemann's organizer is subdivided into two domains by the vegetal alignment zone. Development 124, 895–906.

Latinkic, B.V., Smith, J.C., 1999. *Goosecoid* and *Mix.1* repress *Brachyury* expression and are required for head formation in *Xenopus*. Development 126, 1769–1779.

Manes, M.E., Casal, F.C., 1997. Inductive interactions required for mesodermal differentiation in *Bufo arenarum* gastrula. Dev. Genes Evol. 207, 90–96.

Mangold, O., 1933. Über die Induktionsfähighkeit der verschiedenen Bezirke der Neurula von Urodelen. Naturwissenshaften 21, 761–766 (in German).

Mizuno, M., Takabatake, T., Takahashi, T.C., Takeshima, K., 1997. *Pax-6* gene expression in newt eye development. Dev. Genes Evol. 207, 167–176.

Muhr, J., Jessell, T.M., Edlund, T., 1997. Assignment of early caudal identity to neural plate cells by a signal from caudal paraxial mesoderm. Neuron 19, 487–502.

Nieuwkoop, P.D., 1996. What are the key advantages and disadvantages of urodele species compared to anuran as a model system for experimental analysis of early development? Int J. Dev. Biol. 40, 617–619.

Nieuwkoop, P.D., Florschütz, P.A., 1950. Quelques caracteres speciaux de lagastrulation et de la neurulation de l'oeuf de *Xenopus laevis*, Daud. et de quelques autres anoures. Arch. Biol. 61, 113–150 (in French).

Nieuwkoop, P.D., Boterenbrood, E.C., Kremer, A., Bloemsma, F.F.S.N., Hoessels, E.L.M.J., Meyer, G., Verheyen, F.J., 1952. Activation and Organization of the central nervous system in amphibians. I. Induction and activation. II. Differentiation and organization. III. Synthesis of a new working hypothesis. J. Exp. Zool. 120, 83–108.

Ninomiya, H., Elinson, R.P., Winklbauer, R., 2004. Antero-posterior tissue polarity links mesoderm convergent extension to axial patterning. Nature 430, 364–367.

Okada, Y.K., Hama, T., 1945. Regional differences in the inductive capacity of the dorsal roof of the archenteron of the urodele, *Triturus (Cynops) pyrrhogaster*. Proc. Japan Acad. 21, 240–247 (available online, Journal@chive, Japan Science and Technology Agency).

Okada, Y.K., Ichikawa, M., 1947. A new normal table of the development of *Triturus* (*Cynops*) *pyrrhogaster*. Jpn. J. Exp. Morphol. 3, 1–6.

Pollet, N., Muncke, N., Verbeek, B., Li, Y., Fenger, U., Delius, H., Niehrs, C., 2005. An atlas of differential gene expression during early *Xenopus* embryogenesis. Mech. Dev. 122, 365–439.

Poznanski, A., Minsuk, S., Stathopoulos, D., Keller, R., 1997. Epithelial cell wedging and neural trough formation are induced planarly in *Xenopus*, without persistent vertical interactions with mesoderm. Dev. Biol. 189, 256–269.

Saha, M.S., Grainger, R.M., 1992. A labile period in the determination of the anterior–posterior axis during early neural development in *Xenopus*. Neuron 8, 1003–1014.

Sakaguchi, K., Kaneda, T., Matsumoto, M., Imoh, H., Suzuki, A.S., 2002. Establishment of the organizing activity of the lower endodermal half of the dorsal marginal zone is a primary and necessary event for dorsal axis formation in *Cynops pyrrhogaster*. Int. J. Dev. Biol. 46, 793–800.

Sakami, S., Hisatomi, O., Sakakibara, S., Liu, J., Reh, T.A., Tokunaga, F., 2005. Downregulation of *Otx2* in the dedifferentiated RPE cells of regenerating newt retina. Dev. Brain Res. 155, 49–59.

Shin, J., Keller, R., 1992. The epithelium of the dorsal marginal zone of *Xenopus* has organizer properties. Development 116, 887–899.

Shook, D.R., Keller, R., 2008. Morphogenic machines evolve more rapidly than the signals that pattern them: lessons from amphibians. J. Exp. Zool. (Mol. Dev. Evol.). 310B, 111–135.

Smith, J.C., Price, B.M., Green, J.B., Weigel, D., Herrmann, B.G., 1991. Expression of a *Xenopus* homolog of *Brachyury (T)* is an immediate-early response to mesoderm induction. Cell 67, 79–87.

Sone, K., Takeshima, K., Takahashi, T.C., Takabatake, T., 1997. Temporal alteration of dose-dependent response to activin in newt animal-cap explants. Dev. Genes Evol. 207, 147–155.

Stewart, R.M., Gerhart, J.C., 1991. Induction of notochord by the organizer in *Xenopus*. Roux's Arch. Dev. Biol. 199, 341–348.

Suzuki, A., Kuwabara, K., Kuwabara, Y., 1975. Temporal relations between extension of archenteron roof and realization of neural induction during gastrulation of newt embryo. Dev. Growth Differ. 17, 343–353.

Suzuki, A.S., Mifune, Y., Kaneda, T., 1984. Germ layer interactions in pattern formation of amphibian mesoderm during primary embryonic induction. Dev. Growth Differ. 26, 81–94.

Suzuki, A.S., Sakaguchi, K., Tajima, T., Sasaki, T., Imoh, H., 2002. Study of *Cynops* notochord differentiation using a novel monoclonal antibody. Dev. Growth Differ. 44, 127–134.

Takabatake, T., Takahashi, T.C., Inoue, K., Ogawa, M., Takeshima, K., 1996. Activation of two *Cynops* genes, *Folk Head* and *Sonic hedgehog*, in animal cap explants. Biochem. Biophis. Res. Com. 218, 395–401.

Takaya, H., 1978. Dynamics of the organizer. Morphogenetic movements and specificities in induction and differentiation of the organizer. In: Nakamura, O., Toivonen, S. (Eds.), Organizer—a Milestone of a Half-century from Spemann. Elsevier/North Holland Biomedical Press, pp. 49–70.

Wacker, S.A., Jansen, H.J., McNulty, C.L, Houtzagen, E., Durston, A.J., 2004. Timed interactions between the *Hox* expressing non-organiser mesoderm and the Spemann organiser generate positional information during vertebrate gastrulation. Dev. Biol. 268, 207–219.

Wilson, S.I., Edlund, T., 2001. Neural induction: toward a unifying mechanism. Nature Neuroscience supplement 4, 1161–1168.

Wilson, L., Maden, M., 2005. The mechanisms of dorsoventral patterning in the vertebrate neural tube. Dev. Biol. 282, 1–13.

Winklbauer, R., Schürfeld, M., 1999. Vegetal rotation, a new gastrulation movement involved in the internalization of the mesoderm and endoderm in *Xenopus*. Development 126, 3703–3713.

Vodicka, M.A., Gerhart, J.C., 1995. Blastomere derivation and domains of gene expression in the Spemann organizer of *Xenopus laevis*. Development 121, 3505–3518.

Vogt, W., 1929. Gestaltungsanalyse am Amphibienkeim mit örtlicher Vitalfärbung. II Teil: Gastrulation und Mesodermbildung bei Urodelen und Anuren. W. Roux' Arch. EntwMech. Org. 120, 384–706 (Translated into Japanese by T. Hama, 1992. "Morphogenetic movement and organogenesis in the amphibian embryos", Gakkai Shuppan Center, Tokyo).

Vonica, A., Gumbiner, B.M., 2007. The *Xenopus* Nieuwkoop center and Spemann–Mangold organizer share molecular components and a requirement for maternal *Wnt* activity. Dev. Biol. 312, 90–102.

Yamamoto, Y., Suzuki, A.S., 1994. Two essential processes in the formation of a dorsal axis during gastrulation of *Cynops* embryo. Roux's Arch. Dev. Biol. 204, 11–19.

Yokota, C., Ariizumi, T., Asashima, M., 1998. Patterns of gene expression in the core of Spemann's organizer and activin-treated ectoderm in *Cynops pyrrhogaster*. Dev. Growth Differ. 40, 335–341.

Youn, B.W., Keller, R.E., Malacinski, G.M., 1980. An atlas of notochord and somite morphogenesis in several anuran and urodelean amphibians. J. Embryol. Exp. Morph. 59, 223–245.

Zoltewicz, J.S., Gerhart, J.C., 1997. The Spemann organizer of *Xenopus* is patterned along its anteriorposterior axis at the earliest gastrula stage. Dev. Biol. 192, 482–491.